Fibers and Polymers 2015, Vol.16, No.10, 2284-2293
DOI 10.1007/s12221-015-5507-3

ISSN 1229-9197 (print version)
ISSN 1875-0052 (electronic version)

Effect of Microcrystalline Cellulose on Biodegradability, Tensile and Morphological Properties of Montmorillonite Reinforced Polylactic Acid Nanocomposites

Reza Arjmandi, Azman Hassan*, M. K. Mohamad Haafiz[1]*, and Zainoha Zakaria[2]

Department of Polymer Engineering, Faculty of Chemical Engineering, Universiti Teknologi Malaysia, Johor Bahru 81310, Malaysia

[1]*School of Industrial Technology, Universiti Sains Malaysia, Penang 11800, Malaysia*

[2]*Faculty of Science, Universiti Teknologi Malaysia, Johor Bahru 81310, Malaysia*

(Received July 6, 2015; Revised August 9, 2015; Accepted August 19, 2015)

Abstract: The objective of this study is to investigate the effects of incorporating microcrystalline cellulose (MCC) on montmorillonite (MMT) reinforced polylactic acid (PLA) nanocomposites prepared by solution casting method. The biodegradability, tensile and morphological properties of PLA hybrid composites were investigated using soil burial test, tensile testing machine, field emission scanning electron microscopy, transmission electron microscopy (TEM) and optical microscopy. In addition, Fourier transform infrared spectroscopy (FTIR) was used to observe the interactions between fillers and PLA in the hybrid composites. Various amounts of MCC were added to the optimum formulation which was 5 phr of MMT to produce PLA/MMT/MCC hybrid composites. The biodegradability of hybrid composites increased compared to nanocomposite with 5 phr MMT content and neat PLA. Interestingly, the ductility of PLA/MMT/MCC hybrid composites increased significantly with the addition of 1 phr MCC filler. FTIR analysis revealed some interactions between PLA and both fillers in the hybrid composites. X-ray diffraction and TEM analyses revealed that incorporation of MCC filler into optimum formulation of PLA/MMT nanocomposites slightly decreased the interlayer spacing of MMT in the PLA/MMT/MCC hybrid composites.

Keywords: Biodegradability, Hybrid composites, Polylactic acid, Microcrystalline cellulose, Montmorillonite

Introduction

Biopolymers deserve earnest consideration and among the biopolymers, polylactic acid (PLA) is one of the most studied biodegradable biopolymers [1,2]. Due to increasing concern over environmental issues as well as diminishing petrochemical resources, there is a constant growing interest in the polymer research community in the production and development of plant based biodegradable biopolymers for a wide variety of applications [3-5]. PLA is a biodegradable thermoplastic polyester produced from lactic acid, which is derived from the fermentation of sugar feed stocks such as corn starch [6-8]. PLA has become popular as a biodegradable plastic because of its high stiffness and easy processability compared to other biodegradable polymers. The properties of PLA are generally considered to be comparable to common non-biodegradable thermoplastics like polystyrene (PS) and polyethylene terephthalate (PET) [9]. In spite of these advantages, the applicability of PLA is still limited by its high production cost, brittleness, low water vapor/gas barrier properties and low thermal stability [3,10]. To overcome the inherent limitations of PLA many techniques have been adopted, including blending with other biodegradable polymers and also the development of composites and nanocomposites containing high aspect ratio of organic and inorganic fillers.

*Corresponding author: azmanh@cheme.utm.my
*Corresponding author: mhaafiz@usm.my

PLA nanocomposites based on layered silicates are popular among scientists and in various industries. Researches on PLA nanocomposites reinforced with layered silicates have been carried out extensively and the results have proved that PLA/layered silicates nanocomposites display significant improvements in thermal stability, mechanical toughness, resistance to flammability, crystallization rate, and reduced permeability to small molecules [11,12]. Among the layered silicates, montmorillonite (MMT) is a promising nanofiller due to its easy availability, non-toxicity, low cost, stiffness, high aspect ratio and relative ease of processability [13,14]. Due to its hydrophilicity, MMT does not interact strongly with hydrophobic polymers such as PLA. Thus, to increase its dispersion in polymer matrices, MMT is often treated with organic surfactants such as octadecylamine. The treated MMT is suitable as fillers for nanocomposites and is particularly attractive because of the potential to fine-tune its surface chemistry through ion exchange reactions with organic and inorganic cations [15]. Furthermore, because MMT particles with nanoscale layered structure have a high surface area, their incorporation in polymer nanocomposites produces extensive interfacial regions that lead to tremendous improvements in a wide range of physical and engineering properties compared to neat PLA [15,16]. PLA/MMT nanocomposites have been reasonably well studied for melt processing and solution casting applications [17,18], although different optimum values for MMT content have been reported (≤5 wt%). In a recent study by Arjmandi *et al*. [19]

it was found that the optimum MMT content is 5 parts per hundred parts of polymer (phr), based on formulation which gave the highest tensile strength. Unfortunately, despite the benefits of MMT, ductility is detrimentally affected by the addition of MMT. To minimize production costs for fully biodegradable polymer nanocomposites, PLA/MMT nanocomposites with the addition of low price, renewable and biodegradable material, such as cellulose, is a promising approach which also lead to increases the biodegradation rate of PLA [20].

Previously, it has been reported that the use of cellulose, which is a naturally abundant material, can reduce production costs and also enhance the mechanical properties, biodegradability and thermal stability of PLA [21-23]. Although cellulose can be obtained from a wide variety of sources such as plants, algae, marine creatures and bacteria, the obtained cellulose from cotton contains the highest percentage of cellulose compared to other sources (>95 %). A single cotton fiber (thickness: 20-30 μm) is comprised of superfine fibrils with nanometer scale diameters [24]. One of the cellulose fillers that could be used to filled a polymer matrix is microcrystalline cellulose (MCC) [25,26]. MCC is produced from natural cellulose through a combination of mechanical and chemical processing [27,28]. The degree of crystallinity displayed by MCC, which typically ranges from 55-80 %, depends on the source of the cellulose as well as processing variables such as the reaction temperature and duration, the drying conditions and the extent mechanical agitation applied to the slurry [29,30]. In general, the degree of crystallinity is one of the most important properties that influences the performance of cellulose and its derivatives in various applications. Therefore, MCC has great potential for use as a biodegradable filler in polymer composites. To date, a few researchers have investigated PLA/MCC composites and improvements in stiffness have been achieved through the addition of MCC [28]. According to Petersson and Oksman [7], the PLA/layered silicate showed significant improvements in both tensile modulus and yield strength, while the PLA/MCC composite only improved the yield strength. However, they also found that these two materials had different effects on the elongation at break. The MCC showed a more satisfactory elongation at break behavior compared to the layered silicate.

Recent publication has reported the effect of cellulose nanowhiskers (CNW) which is nano in size on the mechanical and morphological properties of PLA/MMT nanocomposites [19]. To the best of our knowledge, no study has been reported on the use of MCC fillers to enhance the biodegradability of MMT reinforced PLA nanocomposites. The present study reports the effect of MCC which is micro in size on the biodegradability, tensile and morphological properties of PLA/MMT/MCC hybrid composites prepared by solution casting.

Experimental

Materials

PLA (NatureWork^{TM} PLA 3001D) in pellet form was purchased from NatureWork® LLC (Minnetonka, MN USA). It had a density of 1.24 g cm^{-3} and melt flow index (MFI) of *ca.* 15 g 10 min^{-1} (190 ^{o}C 2.16 kg^{-1}). MCC was supplied by Sigma-Aldrich (Malaysia), Avicel; type PH-101. It was obtained from a cotton linter and had an average particle size of 50 μm. Organo-modified MMT, Nanomer 1.30TC, was obtained from Nanocor Inc. (Arlington Heights IL, USA). Nanomer 1.30TC is organically modified with approximately 30 wt% of octadecylamine and has a mean dry particle size of 16-22 μm. Chloroform was purchased from Merck, Malaysia.

Preparation of PLA Film

10 g of PLA pellets were fully dissolved in 64 m*l* of chloroform by heating in a water bath at 60 ^{o}C for 2 h with constant stirring, as described in recent study by Arjmandi *et al*. [19]. The PLA solution was immediately casted onto clean glass plates and was left at room temperature for 48 h to allow the solvent to evaporate. The thickness of the resulting cast film was approximately 100 μm.

Preparation of PLA/MMT Nanocomposites Film

The PLA/MMT nanocomposites were prepared by mixing 10 g of PLA pellets with MMT at two different concentrations (5 and 7 phr), which PLA nanocomposites with 5 phr MMT content was used as a control sample and 7 phr of MMT content was used to investigate and comparison the morphological properties. The various PLA/MMT mixtures were placed in 64 m*l* of chloroform and stirred with vigorous agitation for 2 hours at 60 ^{o}C until the PLA pellets were fully dissolved. The suspensions were then sonicated using a Bransonic 2510 ultrasonic (2510R-DTH-USA) for 5 minutes and immediately cast onto a clean glass plate, as described above, to obtain composite films of ~100 μm thickness. The composites were designated as P/MT5 and P/MT7 (Table 1).

Table 1. Formulation of PLA nanocomposites and hybrid composites film

Designation	PLA (wt%)	MMT (phr)	MCC (phr)
PLA	100	0	0
P/MT5	100	5	0
P/MT7	100	7	0
P/MT5/MC1	100	5	1
P/MT5/MC3	100	5	3
P/MT5/MC5	100	5	5
P/MT5/MC7	100	5	7

Preparation of PLA/MMT/MCC Hybrid Composites Film

The PLA/MMT/MCC hybrid composites were prepared by mixing 10 g of PLA pellets with 5 phr MMT and different concentrations of MCC (1, 3, 5 and 7 phr). The various PLA/MMT/MCC mixtures were placed in 64 m*l* of chloroform and stirred with vigorous agitation for 2 hours at 60 °C until the PLA pellets were dissolved. After PLA dissolution, the suspensions were sonicated using the same ultrasonic as described earlier for 5 minutes and then immediately cast onto a clean glass plate, as described above, to obtain composite films that were ~100 μm thick. The hybrid composites were designated as P/MT5/MC1, P/MT5/MC3, P/MT5/MC5 and P/MT5/MC7 (Table 1).

Characterization

Biodegradability Analysis

Biodegradation of the neat PLA, P/MT5 nanocomposite and hybrid composites were carried out by soil burial method to stimulate natural composites biodegradation as previously reported by Chuayjuljit *et al*. [31]. Rectangular samples with 25×25×0.1 mm dimensions were dried in a desiccator until their weights became constant (W_1). The samples were then buried in the compost soil at a depth of 20-25 cm from the surface for 8 weeks. One group of samples were carefully taken out for testing every 14 days, and then washed with distilled water to remove the sand from the surface of samples and dried at 55 °C until their weights became constant (W_2). The percentage of weight loss (%*WL*) was calculated using equation (1).

$$\%WL = [(W_1 - W_2)/W_1] \times 100 \quad (1)$$

Tensile Testing

Instron 4400 Universal Tester from USA was used to measure the tensile strength at the break point for each formulation. The tensile tests were carried out at room temperature according to the ASTM D882-12. A fixed crosshead rate of 12.5 mm min^{-1} was utilized in all cases, and the results were taken as an average of 10 samples.

Fourier Transform Infrared Spectroscopy

Fourier transform infrared spectroscopy (FTIR) was performed using a Perkin Elmer 1600 Infrared spectrometer (USA). All specimens were made into powder and mixed with KBr at a ratio of 1 wt%. Neat KBr was used as IR spectral reference. FTIR spectra of the samples were recorded using Nicolet's AVATAR 360 at 32 scans with a resolution of 4 cm^{-1} and within the wave range of 4000 to 370 cm^{-1}.

Morphology Analysis

The morphologies of samples were characterized by field emission scanning electron microscopy (FESEM), transmission electron microscopy (TEM) and optical microscopy (OM). FESEM was conducted on a Carl Zeiss (Germany) Supra 35 VP using an extra high tension (EHT) of 8-10 kV. The samples were sputter-coated with gold prior to observation. The microstructure of PLA composites and the filler dispersion in the matrix were investigated using TEM (JEOL JEM-2010, USA). Samples for TEM analysis were sectioned with an ultra-microtome (RMC, model MTXL) to obtain 70 nm thick slices.

OM was used to analyze the microstructure of the MMT and MMT/MCC hybrid fillers in the PLA. Images of the samples were obtained using an ECLIPSE E800-Nikon microscope (USA) equipped with a DXM1200F-Nikon camera. These analyses were carried out at room temperature. Optical images of composites were taken at multiple locations on the sample surfaces.

X-ray Diffraction

X-ray diffraction (XRD) analysis was performed on a Siemens (Berlin, Germany) D5000 X-ray diffractometer. The diffraction patterns were recorded with a step size of 0.02°, from 2θ=2.0 to 10.0°. The interlayer distances (*d*-spacing) of the MMT in the nanocomposites and hybrid composites were derived from the peak positions in the XRD patterns, according to Bragg's Law. The interlayer distances of materials were calculated using equation (2).

$$d\text{-spacing} = n\lambda / 2\sin\theta \quad (2)$$

where n is an integer, θ is the diffraction angle giving the primary diffraction peak, and λ is the X-ray wavelength. In these experiments, λ=0.15406 nm (Cu Kα) and n=1 were used.

Results and Discussion

Biodegradability

The biodegradability of neat PLA, P/MT5 nanocomposite and PLA/MMT/MCC hybrid composites were investigated using soil burial method. The weight loss percentage (%*WL*) of neat PLA, P/MT5 nanocomposite and hybrid composites are shown in Table 2. In addition, Figure 1 shows the images of the samples prior and after soil burial test. As can be observed from Table 2, the weight loss percentage of the samples is dependent on the MCC content, which increased with increasing MCC content in the hybrid composites

Table 2. Percentage weight loss of the neat PLA, P/MT5 nanocomposite and PLA/MMT/MCC hybrid composites after soil burial

Samples	Percentage of weight loss (%*WL*)			
	2 Weeks	4 Weeks	6 Weeks	8 Weeks
PLA	0.13	0.26	0.36	0.45
P/MT5	0.39	0.43	0.53	0.64
P/MT5/MC1	0.91	0.99	1.18	1.35
P/MT5/MC3	1.05	1.22	1.39	1.74
P/MT5/MC5	1.25	1.44	1.58	1.89
P/MT5/MC7	1.45	1.63	1.84	2.10

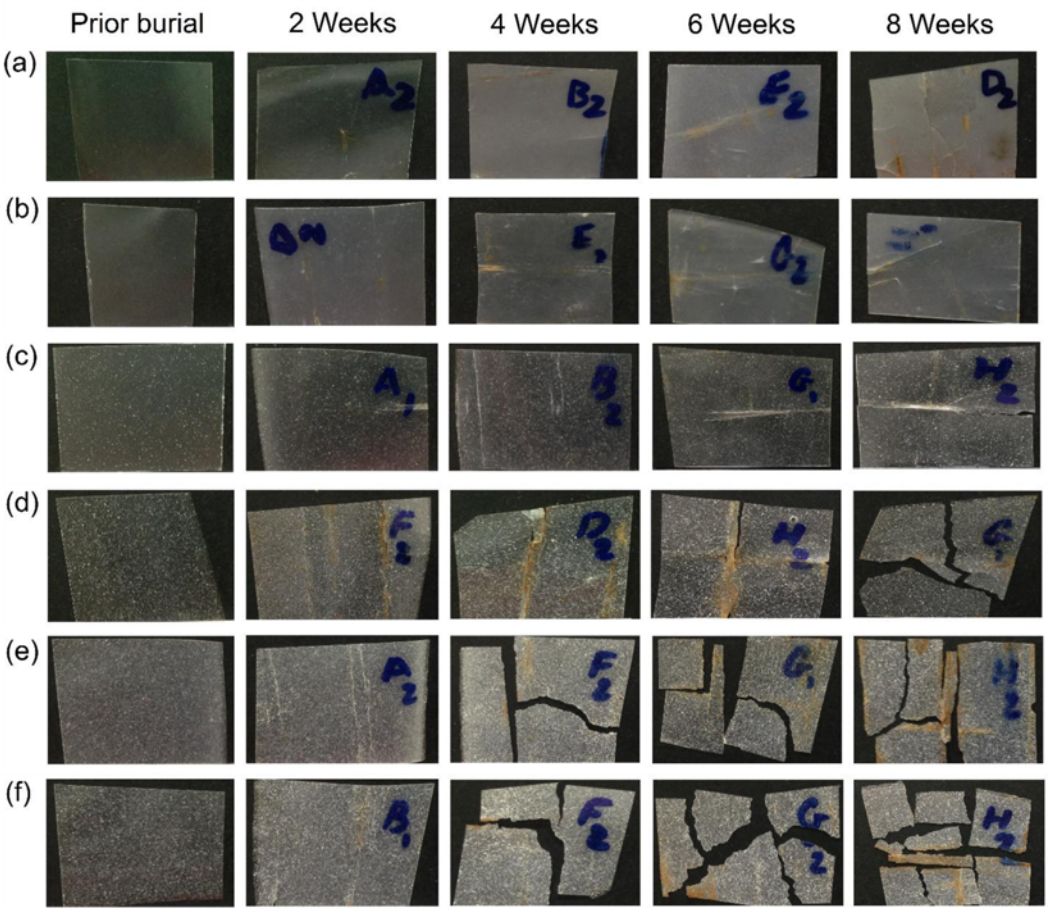

Figure 1. Biodegradables images of the hybrid composites samples prior and after soil burial test; (a) neat PLA, (b) P/MT5 nanocomposite, (c) P/MT5/MC1, (d) P/MT5/MC3, (e) P/MT5/MC5, and (f) P/MT5/MC7 hybrid composite.

compared to the P/MT5 nanocomposite and neat PLA. This suggests that the microorganisms such as fungi were consumed cellulose materials on the surface of samples as a nutrient source, resulted in increased weight loss percentage [31]. As can be clearly seen in Figure 1, no single hole or crack can be observed on the surface of P/MT5 nanocomposite and neat PLA up to week 6th. However, the P/MT5 nanocomposite and neat PLA started to show some cracks in week 8th. The changes on the surface of hybrid composites were observed from week 4th, where the samples started to show the initial cracks. Interestingly, prolonging the burial time led to higher degradation of hybrid composites. Due to the higher degradation rate of MCC fillers compared to PLA, formation of crack is faster which led to an increase in the weight loss of the samples. It can be concluded that the addition of MCC into P/MT5 nanocomposite increased the biodegradability of PLA. Similar observations were reported by Mathew *et al*. [28] and Bras *et al*. [32], when MCC and CNW were incorporated into PLA and natural rubber as fillers, respectively. They found that the presence of MCC and CNW enhanced the biodegradation of PLA and rubber in soil because of faster degradation rate of cellulose compared to PLA and natural rubber. In addition, Arjmandi *et al*. [33] studied the effect of partial replacement of MMT with CNW on the properties of PLA. They found that the percentage of weight loss of the PLA hybrid nanocomposites increased with increasing CNW content. Besides that, the percentage of weight loss increased with increasing burial time which is consistent with the present study.

Tensile Properties

The effect of MMT content on the tensile strength and elongation at break of PLA/MMT nanocomposites is reported in earlier publication by Arjmandi *et al*. [19]. It was reported that the addition of MMT into PLA increased the tensile strength of the nanocomposites films and reached a maximum value at 5 phr MMT content. Figure 2 shows the effect of MCC content on the tensile strength and elongation at break of PLA/MMT/MCC hybrid composites, since these two properties are the most important properties among the mechanical properties for food packaging application. The introduction of MCC resulted in a decrease in tensile strength

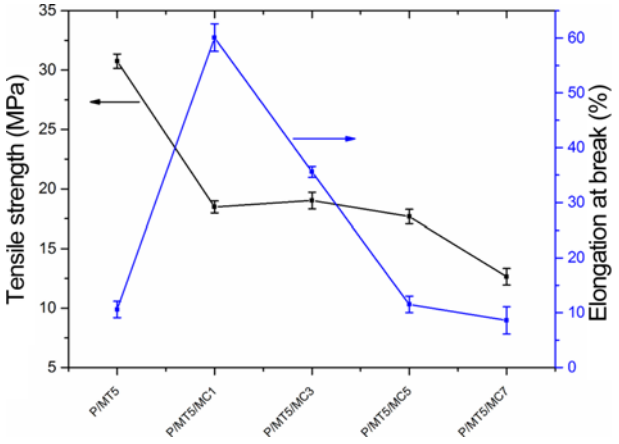

Figure 2. Tensile strength and elongation at break of PLA/MMT/MCC hybrid composites.

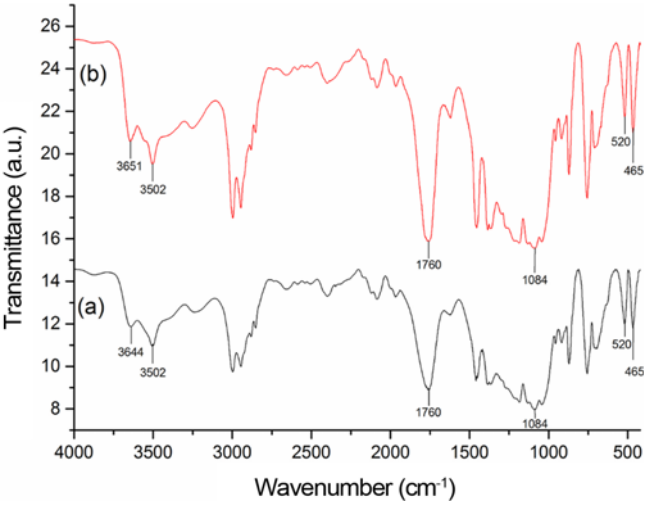

Figure 3. FTIR spectra of (a) P/MT5 nanocomposite [20] and (b) P/MT5/MC1 hybrid composite.

for the hybrid composites. The addition of MCC resulted in approximately 38 % lower tensile strength compared to PLA/MMT at 5 phr MMT content. This decrease could be due to the agglomeration of MCC in the PLA induced by Van der Waal's forces.

In contrast, the addition of 1 phr MCC into PLA/MMT to form PLA/MMT/MCC hybrid composites increased the elongation at break from approximately 10 to 60 % (Figure 2), which is rather significant. This increase in elongation at break is not surprising, since Petersson and Oksman [7] reported that MCC was much better than layered silicate in terms of maintaining elongation at break values. However, the elongation at break decreased with further addition of MCC. The initial increase in elongation at break with the addition of 1 phr MCC into the hybrid composites could potentially be attributed to MCC reducing the ability of MMT to restrict the mobility of polymer chains. Nevertheless, the addition of a similar amount of MCC reduced the tensile strength significantly due to the poor adhesion of MCC to PLA. Thus, it can be said that, at this filler content, poor adhesion is detrimental to tensile strength but not to ductility. Interestingly, although the elongation at break of hybrid composites with 3 phr MCC was lower than hybrid composites with 1 phr MCC, the elongation at break of P/MT5/MC3 hybrid composites was still higher than P/MT5 nanocomposites. This result suggests that MCC may play an important role in increasing the ductility of PLA/MMT nanocomposites.

FTIR Spectroscopy Analysis

FTIR spectroscopy was used to observe the interactions between fillers and PLA matrix. FTIR spectra of P/MT5 nanocomposite and P/MT5/MC1 hybrid composite are shown in Figures 3(a) and (b), respectively. The peaks at 465 and 520 cm^{-1} (Figure 3(a)) are attributed to the absorption peaks of Si-O vibrations [34]. As can be seen in Figure 3(b), the stretching vibration peaks of O-H, C=O and C-O were shifted to the lower wave numbers (3502, 1760 and 1084 cm^{-1}, respectively) compared to the similar peaks in the FTIR spectra of neat PLA [19]. These shifts are attributed to the possibility of some interactions between the hydroxyl groups of the PLA and the hydroxyl groups of the ammonium surfactant in the organically modified MMT. These shifts are also attributed to the interactions between the carbonyl groups of PLA and the hydroxyl groups of MMT.

In addition, interactions between the hydroxyl groups of PLA and the Si-O groups of MMT could have also contributed to these shifts. Similar findings were previously reported by Chen *et al*. [34] and Liu *et al*. [35]. No new peak was observed when MCC was added to PLA/MMT nanocomposites (Figure 3(b)). The absence of new peak suggest that MCC filler used to produce the hybrid composites film only physically interacted with PLA rather than chemical interactions. This result is similar to the one reported by Qu *et al*. [36]. Interestingly, however, the intensity of the peaks at 3502 and 3651 cm^{-1} were increased by the addition of 1 phr MCC to the P/MT5 nanocomposite (Figure 3(b)). Additionally, the peak that appeared at 3644 cm^{-1} in P/MT5 (Figure 3(a)) shifted to a higher wave number (3651 cm^{-1}) in P/MT5/MC1 hybrid composite (Figure 3(b)), due to the possibility of some interactions between the carbonyl groups of PLA and the hydroxyl groups of MCC. Furthermore, interactions between the hydroxyl groups of PLA and hydroxyl groups of MCC could have also contributed to this shift. In summary, these results indicated that some interactions occurred between the PLA and both MMT and MCC.

Field Emission Scanning Electron Microscopy

Figure 4 shows FESEM images of fractured cross-sectional surfaces of PLA/MMT nanocomposites and PLA/MMT/MCC hybrid composites. The fractured cross-sectional surfaces

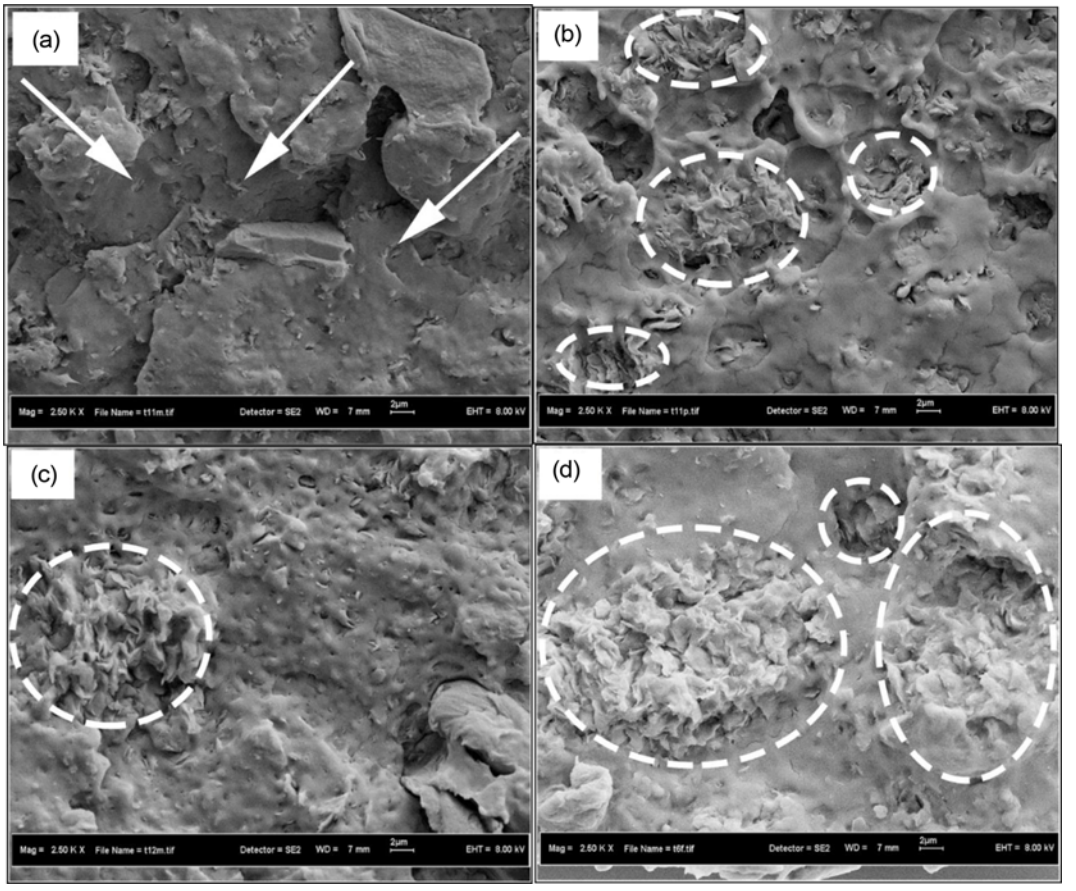

Figure 4. FESEM micrographs of fractured cross-sections of (a) P/MT5 nanocomposite, (b) P/MT7 nanocomposite, (c) P/MT5/MC1 hybrid composite, and (d) P/MT5/MC3 hybrid composite.

of P/MT5, P/MT7, P/MT5/MC1 and P/MT5/MC3 are shown in Figures 4(a)-(d), respectively. Figure 4(a) clearly shows that MMT fillers are dispersed uniformly throughout the PLA due to its finer particle size and that MMT fillers are embedded within the PLA at 5 phr MMT content. As the MMT content increased (Figure 4(b)), agglomeration of MMT particles can be observed (indicated by the circle). Similar findings were reported by Chang *et al*. [18] as aggregated MMT was found at high concentrations of MMT (>5 wt%). Figure 4(c) shows the fractured cross-sectional surfaces of a P/MT5/MC1 hybrid composite. The addition of MCC (1 phr) into P/MT5 nanocomposite clearly led to agglomeration of MCC, which is indicated by the circle. This agglomeration likely resulted in the decreased tensile strength that was observed for hybrid composites compared to P/MT5 nanocomposites. It can be observed from Figure 4(d) that the aggregation of MCC increased as the MCC content into the P/MT5 nanocomposite was increased (as shown by circle). Similar results were observed by Mathew *et al*. [28] and Haafiz *et al*. [29] when MCC was added into PLA using melt extrusion process and solution casting, respectively.

Transmission Electron Microscopy

TEM images of the PLA composites reinforced with MMT and MMT/MCC are shown in Figure 5. Figure 5(a) displays a TEM micrograph of P/MT5 nanocomposite. It clearly shows that the layered MMT is separated in the PLA. The spaces between the dark lines are the interlayer space (white arrows), and the grey bases correspond to the PLA, as indicated by the red arrow. Similar observations were reported by Chang *et al*. [18] and Chang *et al*. [37] when PLA was reinforced with MMT filler. This result, along with the XRD data that will be discussed in XRD section, demonstrates that PLA/MMT nanocomposites with 5 phr MMT formed an intercalated structure system. As the MMT content increased (Figure 5(b)), agglomeration of MMT layered silicates can be observed (indicated by the arrows). Figure 5(c) shows TEM micrograph of P/MT5/MC1 hybrid composite. It can be observed that the MCC fillers are unevenly dispersed and caused the MCC particles to agglomerate (indicated by the circle). Dispersed layers of MMT can also be observed in Figure 5(c), as indicated by the arrows. Similar results were reported by Cheng *et al*. [38] for PLA reinforced with hybrid aluminum trihydrate

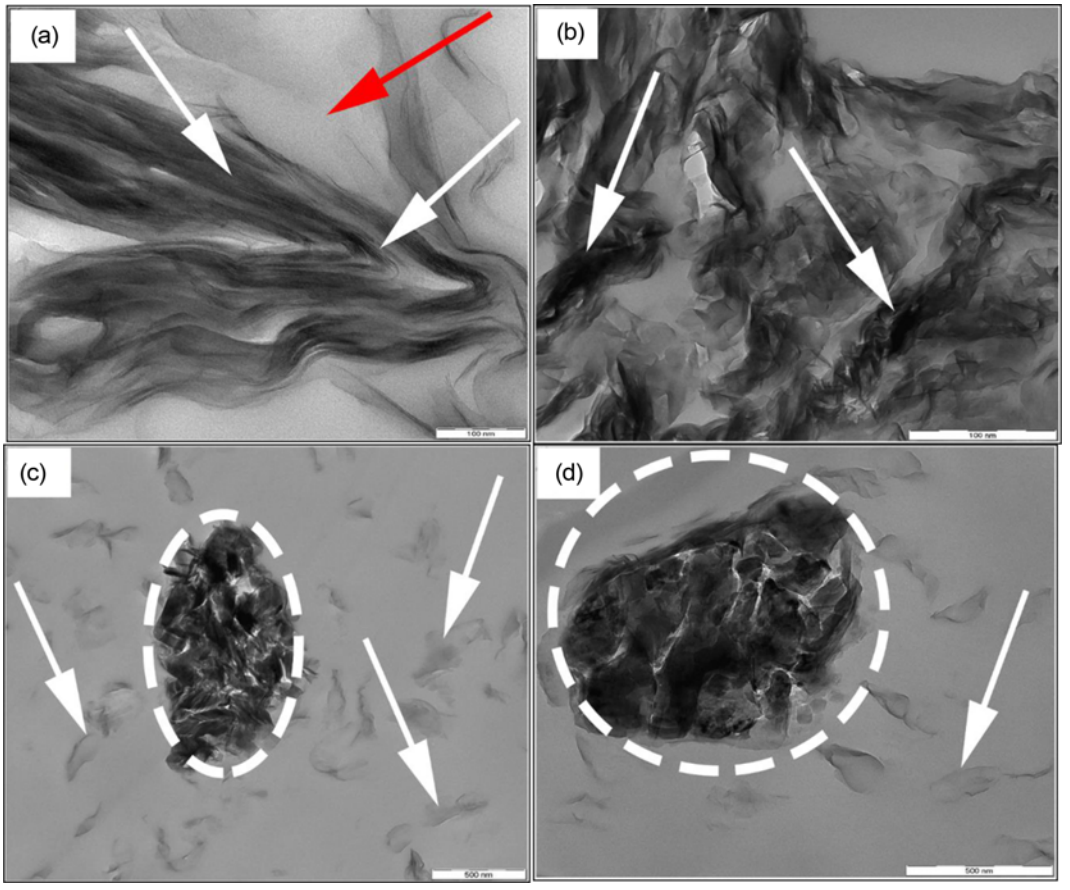

Figure 5. TEM micrographs of (a) P/MT5 nanocomposite, (b) P/MT7 nanocomposite, (c) P/MT5/MC1 hybrid composite, and (d) P/MT5/MC3 hybrid composite.

(ATH)/MMT fillers. Figure 5(c) shows that MCC particles affect the intercalation of MMT platelets, leading to fewer intercalated MMT platelets in the hybrid composites compared to P/MT5 nanocomposites. From Figure 5(d), it can be observed that the aggregation of MCC increased as the MCC content into the P/MT5 nanocomposite increased, as indicated by the circle.

Optical Microscopy

To further investigate the MMT and MMT/MCC dispersion in the PLA, the surfaces of PLA/MMT nanocomposites and PLA/MMT/MCC hybrid composites films were characterized by optical microscopy. Figures 6(a)-(d) shows the optical microstructure of P/MT5 nanocomposite, P/MT7 nanocomposite, P/MT5/MC1 and P/MT5/MC3 hybrid composites, respectively. Figure 6(a) shows that MMT fillers are well dispersed in the PLA at 5 phr MMT content. However, as the MMT content increased (Figure 6(b)), aggregation of MMT can be observed, similar to the FESEM and TEM analysis as discussed above. Similar observations were reported by Cyras *et al*. [39] and Ranade *et al*. [40] where MMT was added to starch and polyethylene (PE) matrices, respectively. Additionally, in the image of the P/MT5/MC1 hybrid composite (Figure 6(c)), the black spots are the MMT platelets (indicated by the arrows) and the agglomerations correspond to the MCC in the PLA (indicated by the circles). Similar observations for MCC particles in a PLA were made by Mathew *et al*. [28]. The sizes of the MCC particles were approximately 10 to 20 μm in thickness and approximately 50 μm in length. The MCC filler did not uniformly disperse within the PLA, and the aggregation of MCC on the surface of hybrid composites was readily apparent. Figure 6(d) shows that increasing the MCC content further increased the agglomeration of MCC (indicated by the arrows) in the hybrid composites. This result is consistent with that obtained by FESEM and TEM analyses.

X-ray Diffraction

The XRD patterns of MMT, P/MT5 nanocomposite and P/MT5/MC1 hybrid composite are shown in Figure 7. The values of $2\theta^{\circ}$ and their relative *d*-spacing are also presented in Table 3. MMT showed a diffraction peak at 2θ=4.15°, which corresponds to a *d*-spacing of 2.14 nm for the 001 peak (*d*-spacing and diffraction angle θ are related through

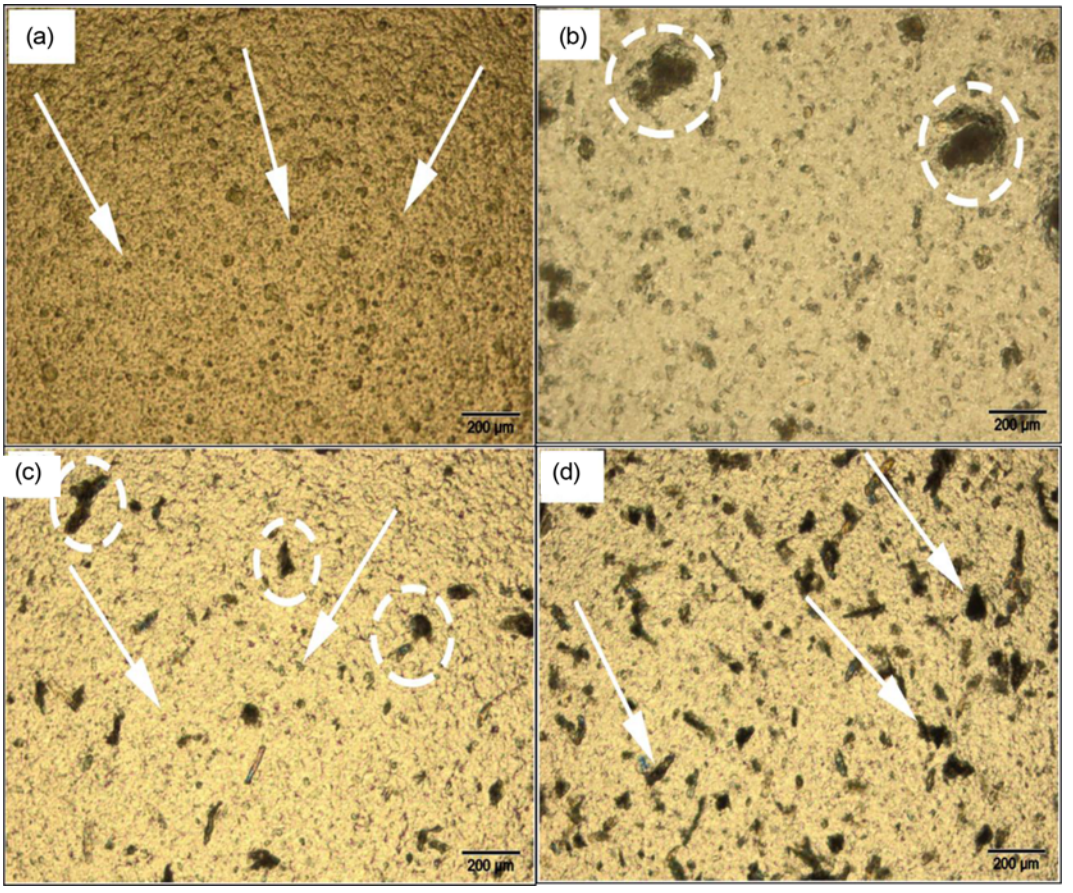

Figure 6. OM micrographs of (a) P/MT5 nanocomposite, (b) P/MT7 nanocomposite, (c) P/MT5/MC1 hybrid composite, and (d) P/MT5/MC3 hybrid composite.

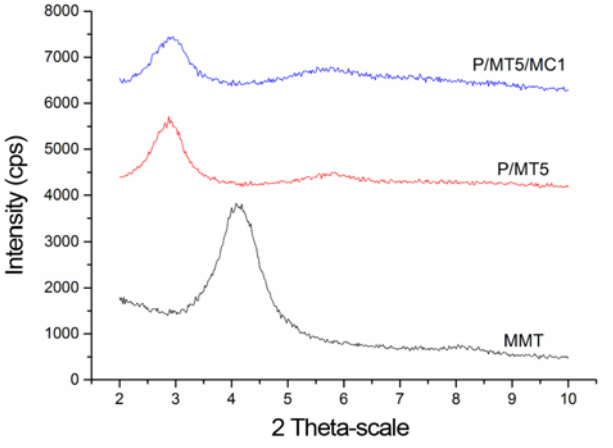

Figure 7. XRD patterns of MMT, P/MT5 nanocomposite and P/MT5/MC1 hybrid composite.

Bragg's equation "$n\lambda=2d\sin\theta$" where λ is the wavelength of X-ray). XRD pattern of PLA nanocomposite with 5 phr MMT content (Figure 7) showed a (001) peak at lower angles compared to the XRD pattern of MMT. As shown in Figure 7, the diffraction peak attributed to the (001) reflection in the P/MT5 nanocomposite is at $2\theta=2.82^{\circ}$, which corresponds to a *d*-spacing of 3.15 nm. The appearance of peaks at lower diffraction angles and larger *d*-spacing suggests the presence of structures with limited interactions, and can be attributed to the formation of nanocomposites. This result also shows the scattering and dispersion of the MMT nanolayers within the PLA and indicates the formation of an intercalated nanostructure, similar to previously reported studies [7,41]. This observation from XRD is consistent with the TEM analysis of PLA nanocomposites in which 5 phr MMT produced intercalated nanocomposites (Figure 5(b)).

The increase in interlayer spacing of MMT may be due to

Table 3. The 2θ angle and *d*-spacing of MMT, P/MT5 nanocomposite and P/MT5/MC1 hybrid composite

Sample	MMT	P/MT5	P/MT5/MC1
	001	001	001
$2\theta^{\circ}$	4.15	2.82	2.90
d-spacing (nm)	2.14	3.15	3.08

the organic modification of MMT, which could potentially enable PLA chains to diffuse between the layers during processing [41]. Regardless, the increment in the interlayer spacing of MMT is evidence that PLA polymer chains were intercalated in between the gallery of MMT, as the diffusion of PLA chains in MMT layers would be expected to increase the intergallery distance and reduce the electrostatic attraction between adjacent platelets [42]. Additionally, the intercalation could be attributed to the possibility of some interactions between the fillers and matrix. Previous reports on the distribution of MMT in PLA have shown that the MMT is well dispersed in the PLA. This dispersion could be due to some interactions between ammonium groups in the surfactant of the organically modified MMT and the carbonyl group of the PLA chain segments [7]. In addition, some interactions between the PLA chain hydroxyl groups and MMT platelet surfaces are also possible [11,17].

As shown in Figure 7, the XRD pattern of PLA/MMT/MCC hybrid composites with 5 phr MMT and 1 phr MCC content displayed a slight decrease in *d*-spacing for the 001 peak compared to P/MT5 nanocomposite (from 3.15 to 3.08 nm). This decrease in 001 peak is consistent with the morphological observation, as the addition of MCC in P/MT5 nanocomposites led to MCC agglomeration and reduced intercalation. Although the decrease in *d*-spacing was small, the effect of MCC aggregation can clearly be seen compared to P/MT5 nanocomposites. In general, FESEM and TEM images of the composites correlated well with the XRD results.

Conclusion

PLA/MMT/MCC hybrid composites were prepared by solution casting. Biodegradability of PLA/MMT/MCC hybrid composites increased by the addition of MCC fillers compared to P/MT5 nanocomposite and neat PLA. The rate of weight loss was dependent on the MCC content, whereby the weight loss increased with increasing MCC content. In addition, prolonging the burial time led to higher degradation of hybrid composites. The ductility of hybrid composites containing 1 and 3 phr MCC were higher than P/MT5 nanocomposite. FTIR analysis showed the possibility of some interactions between PLA and both MMT and MCC in the hybrid composites. TEM and XRD analysis provided evidence of the formation of an intercalated structure in the PLA/MMT nanocomposites. However, agglomeration of MCC was readily apparent with the addition of MCC into the PLA/MMT nanocomposites. Due to the presence of agglomerated MCC in hybrid composites, the interlayer spacing of MMT in the hybrid composites slightly decreased, leading to less intercalated MMT platelets in hybrid composites compared to PLA/MMT nanocomposites. It can be concluded that the addition of MCC into nanocomposites increased the biodegradability and elongation at break of the PLA/MMT nanocomposites.

Acknowledgement

The authors would like to acknowledge Universiti Teknologi Malaysia (UTM) and Research University Grant 05H22, sub-code:Q.J130000.2509.05H22 for financial support.

References

1. B. U. Nam, K. D. Min, and Y. Son, *Mater. Lett.*, **150**, 118 (2015).
2. E. Robles, I. Urruzola, J. Labidi, and L. Serrano, *Ind. Crop. Prod.*, **71**, 44 (2015).
3. M. D. Sanchez-Garcia and J. M. Lagaron, *Cellulose*, **17**, 987 (2010).
4. S. Y. Cho, H. H. Park, Y. S. Yun, and H. J. Jin, *Fiber. Polym.*, **14**, 1001 (2013).
5. M. R. Kaiser, H. B. Anuar, N. B. Samat, and S. B. A. Razak, *Iran. Polym. J.*, **22**, 123 (2013).
6. R. T. De Silva, P. Pasbakhsh, K. L. Goh, S. P. Chai, and J. J. Chen, *Compos. Mater.*, **48**, 3705 (2013).
7. L. Petersson and K. Oksman, *Compos. Sci. Technol.*, **66**, 2187 (2006).
8. H. Luo, G. Xiong, Q. Li, C. Ma, Y. Zhu, R. Guo, and Y. Wan, *Fiber. Polym.*, **15**, 2591 (2014).
9. L. Petersson, I. Kvien, and K. Oksman, *Compos. Sci. Technol.*, **67**, 2535 (2007).
10. K. Oksman, A. P. Mathew, D. Bondeson, and I. Kvien, *Compos. Sci. Technol.*, **66**, 2776 (2006).
11. M. J. Pluta, *J. Polym. Sci. Pt. B-Polym. Phys.*, **44**, 3392 (2006).
12. J. H. Lee and Y. G. Jeong, *Fiber. Polym.*, **12**, 180 (2011).
13. H. Ferfera-Harrar and N. Dairi, *Iran. Polym. J.*, **23**, 917 (2014).
14. S. A. Attaran, A. Hassan, and M. U. Wahit, *Iran. Polym. J.*, **24**, 367 (2015).
15. S. Sinha Ray and M. Okamoto, *Prog. Polym. Sci.*, **28**, 1539 (2003).
16. Q. H. Zeng, A. B. Yu, G. Q. Lu, and D. R. J. Paul, *Nanosci. Nanotechnol.*, **5**, 1574 (2005).
17. L. Jiang, J. Zhang, and M. P. Wolcott, *Polymer*, **48**, 7632 (2007).
18. J. H. Chang, Y. U. An, and G. S. J. Sur, *J. Polym. Sci. Pt. B-Polym. Phys.*, **41**, 94 (2003).
19. R. Arjmandi, A. Hassan, S. J. Eichhorn, M. K. M. Haafiz, Z. Zakaria, and F. A. Tanjung, *J. Matar. Sci.*, **50**, 3118 (2015).
20. M. Shayan, H. Azizi, I. Ghasemi, and M. Karrabi, *Carbohydr. Polym.*, **124**, 237 (2015).
21. N. Herrera, A. P. Mathew, and K. Oksman, *Compos. Sci. Technol.*, **106**, 149 (2015).
22. X. Wang, P. Qu, and L. Zhang, *Fiber. Polym.*, **15**, 302 (2014).

23. V. S. Karande, A. K. Bharimalla, N. Vigneshwaran, P. G. Kadam, and S. T. Mhaske, *Iran. Polym. J.*, **23**, 869 (2014).
24. P. Satyamurthy, P. Jain, R. H. Balasubramanya, and N. Vigneshwaran, *Carbohydr. Polym.*, **83**, 122 (2011).
25. W. Chen, H. Yu, Y. Liu, P. Chen, M. Zhang, and Y. Hai, *Carbohydr. Polym.*, **83**, 1804 (2011).
26. A. Iwatake, M. Nogi, and H. Yano, *Compos. Sci. Technol.*, **68**, 2103 (2008).
27. J. Lu, T. Wang, and L. T. Drzal, *Compos. Pt. A-Appl. Sci. Manuf.*, **39**, 738 (2008).
28. A. P. Mathew, K. Oksman, and M. Sain, *J. Appl. Polym. Sci.*, **97**, 2014 (2005).
29. M. K. M. Haafiz, A. Hassan, Z. Zakaria, I. M. Inuwaa, M. S. Islam, and M. Jawaid, *Carbohydr. Polym.*, **98**, 139 (2013).
30. S. Chuayjuljit, S. Su-uthai, and S. Charuchinda, *Waste. Manag. Res.*, **28**, 109 (2010).
31. S. Chuayjuljit, S. Hosililak, and A. Athisart, *J. Metal. Mater. Mineral.*, **19**, 59 (2009).
32. J. Bras, M. L. Hassan, C. Bruzesse, E. A. Hassan, N. A. El-Wakil, and A. Dufresne, *Ind. Crop. Prod.*, **32**, 627 (2010).
33. R. Arjmandi, A. Hassan, M. K. M. Haafiz, and Z. Zakaria, *Int. J. Biol. Macromol.*, **81**, 91 (2015).
34. N. L. Chen, H. X. Feng, J. W. Guo, H. M. Luo, and J. H. Qiu, *Adv. Mat. Res.*, **221**, 211 (2011).
35. M. Liu, Y. Zhang, and C. Zhou, *Appl. Clay Sci.*, **75-76**, 52 (2013).
36. P. Qu, Y. Gao, G. Wu, and L. Zhang, *Bioresources*, **5**, 1811 (2010).
37. J. H. Chang, Y. U. An, D. Cho, and E. P. Giannelis, *Polymer*, **44**, 3715 (2003).
38. K. C. Cheng, C. B. Yu, W. Guo, S. F. Wang, T. H. Chuang, and Y. H. Lin, *Carbohydr. Polym.*, **87**, 1119 (2012).
39. V. P. Cyras, L. B. Manfredi, M. T. Ton-That, and A. Vázquez, *Carbohydr. Polym.*, **73**, 55 (2008).
40. A. Ranade, K. Nayak, D. Fairbrother, and N. A. D'Souza, *Polymer*, **46**, 7323 (2005).
41. C. W. Shyang and L. S. Kuen, *Polym. Polym. Compos.*, **16**, 263 (2008).
42. H. Balakrishnan, A. Hassan, M. U. Wahit, A. A. Yussuf, and S. B. A. Razak, *Mater. Des.*, **31**, 3289 (2010).